ELSEVIER

Polymer 42 (2001) 9097–9109

polymer

www.elsevier.com/locate/polymer

Supramolecular self-assembly and opto-electronic properties of semiconducting block copolymers

Bert de Boer, Ulf Stalmach, Paul F. van Hutten, Christian Melzer, Victor V. Krasnikov, Georges Hadziioannou*

Department of Polymer Chemistry, Materials Science Centre, University of Groningen, Nijenborgh 4, NL-9747 AG Groningen, The Netherlands

We dedicate this paper to Prof. Stein in appreciation of his lifelong contribution to science. For many of us, he has been a role model as a human being and educator.

Received 2 March 2001; received in revised form 27 April 2001; accepted 27 April 2001

Abstract

With continuous and nanometre-scale interpenetrating phases of electron donor and acceptor components, a novel diblock copolymer, in which one block is poly(*p*-phenylene vinylene) (PPV) and the other is a C_{60}-functionalized polystyrene, is designed to be an efficient photovoltaic material. The synthesis involves the polymerization of a styrene derivative from a PPV-based macroinitiator via living free radical polymerization, and its subsequent functionalization with C_{60} via atom transfer radical addition. In selective solvents for the polystyrene block, aggregation is detected by means of optical spectroscopy and small-angle neutron scattering. Solid films exhibit honeycomb-structuring at the micrometre level when cast from CS_2. As active layer in a device, the donor–acceptor diblock copolymer shows enhanced photovoltaic response relative to a blend of its constituent polymers.

Keywords: Semiconducting diblock copolymers; Self-organization; Photovoltaic devices

1. Introduction

Research on 'synthetic metals' evolved from a rather esoteric occupation to a lively field of activity ever since the discovery, in 1977, of electrical conductivity in the simple hydrocarbon polymer polyacetylene upon oxidation or reduction (doping) [1,2]. Conjugated polymers, though not the only class of materials known today as 'synthetic metals', now form the most widely investigated group. The dramatic development of this field took off in 1990, after the discovery of electroluminescence in a non-doped conjugated polymer thin film sandwiched between electrodes [3]. As a result, during the 1990s, research in this highly interdisciplinary area has focused on semiconductor rather than conductor properties. Derivatives of polythiophene (PT), poly(*p*-phenylene) (PPP), and poly(*p*-phenylene vinylene) (PPV) are the major candidates for use as the active material in field-effect transistors [4–6], light-emitting diodes [3,7–10], photodetectors [11], photovoltaic cells [12–15], sensors [16], and lasers (solution [17] and solid state [18–21]). Besides their semiconductor properties, polymers also provide a way to obtain patterned structures by means of inexpensive techniques such as spin casting, photolithography [22,23], ink jet printing [24–26], soft lithography [27], screen printing [28] and micromoulding [29] onto almost any type of substrate, including flexible ones [30]. Some applications have already been commercialized (LEDs), while others are certainly technically feasible (plastic solar cells, electronic circuitry). There is good reason to expect that conjugated polymers will play their role in the emerging communication and information technologies, which are based on the use of optical signals for data transfer. The importance of the field of conjugated polymers was recently underlined by awarding the 2000 Nobel Prize in chemistry to the discoverers of conductivity, Heeger, Shirakawa and MacDiarmid.

The main advantage offered by polymers over the traditional semiconductor materials is the versatility of processing methods, which allows a polymer to be obtained in virtually any desired shape and in composite form with many other materials. Deposition as a thin film over a macroscopically large area is particularly attractive. Where classical polymer processing could be used, the processing cost would be low. For this to become a reality, the parent conjugated polymers, which are highly intractable because

* Corresponding author. Fax: +31-50-3634400.
E-mail address: hadzii@chem.rug.nl (G. Hadziioannou).

0032-3861/01/$ - see front matter
PII: S0032-3861(01)00388-3

of their conjugated, inflexible backbone, have to be derivatized without degrading their opto-electronic properties. With clever synthetic chemistry, impressive progress has already been made on this point. An appropriate and well-defined chemical structure is a prerequisite for the control of ultimate properties, but it does not end there. The properties of polymer materials depend sensitively on the details of their processing history, and each step has to be carefully carried out so as to contribute positively to the desired result.

The work described in this paper focuses on polymers for application in photovoltaic cells, which are either light sensor (photodetector) or energy conversion (solar cell) devices. Our emphasis will be on the latter application; in that arena, a well-performing organic material would have to compete with amorphous silicon with regard to energy conversion efficiency (around 10% for a-Si [31]) and fabrication costs. The potential of the polymer clearly lies in the promise of large-area, mechanically flexible, active coatings fabricated by inexpensive processing techniques.

A first requirement for a photovoltaic material is photoconductivity, i.e. that charges are generated upon illumination. Subsequently then, these charges must drift (move in an electric field) towards electrodes for collection. In an organic molecular material, photoexcitation does not directly yield free charge carriers. Due to the low dielectric constant of organics, an electron in the excited state is bound to its vacancy (hole) quite strongly, the binding energy being several tenths of an electronvolt [32]. This bound electron–hole pair is called an exciton. Escape from the Coulomb attraction is promoted by offering an energetically favourable pathway to an electron-accepting molecule. This is the donor–acceptor (D–A) concept, which is commonly applied to organic photovoltaic materials [12]. Dissociation of the exciton, via rapid electron transfer ($<$200 fs [33]), leaves a positively charged donor molecule and a negatively charged acceptor molecule. These are cation and anion species, respectively, stabilized by charge delocalization within their conjugated systems and by polarization of their environment. Exciton dissociation occurs at the interface between donor and acceptor species, a configuration that physicists call the D–A heterojunction. Although it is not a priori evident what the nature of this interface should be in terms of scale and geometry, optimization within the D–A concept is likely to imply that this interface be made large and easily accessible for the excitons generated. Since excitons have a finite lifetime, they have a finite diffusion range as well; hence, the requirement of accessibility naturally leads to constraints for the geometry of the interface. A spatially distributed interface with a correlation length of 10 nm would be compatible with the evolution of the exciton: the exciton would have a higher probability of reaching the interface and dissociate than to decay in another way, e.g. radiatively. After dissociation, the charges must be further separated and transported each through its own phase so as to avoid recombination before the electrode is reached.

It is not obvious how to impose such a nanometre-size and convoluted interface geometry on the mixture of donor and acceptor compounds: they would probably either mix molecularly or phase separate into nearly pure components. This is exactly the point at which block copolymers may provide the answer, because of their ability to self-structure into regular and ordered microphases [34–36]. The simplest concept would be a photovoltaic diblock copolymer consisting of a block with donor functionality linked to a block with acceptor properties. The electronic functions could be either in the main chain of the blocks or in substituents. Microphase separation would produce a suitable geometry at the proper scale that could be fine-tuned via the lengths of the blocks. In this context, cylindrical and bicontinuous interpenetrating morphologies are the most appropriate ones.

From the point of view of structure, there are several intriguing aspects to this approach. The limited solubility of conjugated polymers has been found to lead to aggregation phenomena in various solvents [37,38], which are manifested as changes in their electronic spectra [39,40]. Liquid-crystalline phases have been identified for derivatives of the major types of conjugated polymers [41]. Similar phenomena may occur for a diblock copolymer containing one conjugated block. The presence of one relatively stiff block puts this polymer in the class of rod–coil copolymers. The phase behaviour of rod–coil copolymers has been studied for only a very limited number of systems [42–44] and has turned out to be very different from the now-classical behaviour of flexible diblocks. One may speculate that preferential solvation of the flexible block will lead to the formation of micelle-like aggregates, lyotropic mesophases for the conjugated block, or the like, and that these superstructures will be carried over into the morphology of films cast from such solutions to some degree.

For the application in photovoltaic cells, the combination of a PPV-type polymer or oligomer as the donor material with C_{60} as the acceptor has proven promising [45,46]. While PPVs are fairly good hole conductors, electron transport is poorer, which limits the performance in applications in which PPV is the sole active component. In the two-phase D–A concept for the active layer, as outlined above, this problem is alleviated, since the acceptor transports the electrons. By covalently incorporating C_{60} into a polymer, materials that combine the physical properties of fullerene with the processability of polymers are obtained [47,48] and higher quantities of the acceptor can be accommodated in a finely dispersed form than would be possible for pure C_{60}.

The strategy behind our work having been laid out above, the subsequent sections of this paper will describe the synthesis of a D–A diblock copolymer, its physico-chemical characteristics, its behaviour in solution and its film-forming properties. Finally, our first results on the structural organization of the thin films and their opto-electronic response will be presented.

2. Design and synthesis of a photovoltaic block copolymer

According to the principles discussed above, a self-structuring photovoltaic composite may be formed from a diblock copolymer consisting of a PPV block and a block densely functionalized with C_{60}. For reasons to be described below, the second block will consist of a polystyrene backbone with C_{60} incorporated as substituents. Since conjugated chains are less flexible than conventional polymer chains, conjugated polymers can be regarded as rod-like, and their properties (solubility, phase behaviour) are different from those of polymers such as polystyrene. Hence, our target PPV–PS-based block copolymer belongs to the class of rod–coil copolymers. Most of the rod–coil block copolymers with conjugated polymers or oligomers as the rigid rod synthesized so far [49–56] were obtained by anionic polymerization of the coil polymer, followed by quenching, either with a reactive end-group on the rigid conjugated block or with a functional molecule to obtain an end-functionalized coil polymer that is subsequently coupled to the conjugated block. Conjugated polymers themselves are mostly synthesized by polycondensation reactions. Since polycondensations do not require initiation, growth from a specific site is highly unlikely. Polycondensation from an end-cap on a functionalized polystyrene block, as demonstrated by Jenekhe et al. [52], would require 100% conversion of the polycondensation to circumvent the presence of homopolymer, unless the end-cap is much more reactive than the other reactive groups.

The exclusive use of anionic polymerization techniques to obtain rod–coil block copolymers was demonstrated by Leclère et al. [55]. They anionically polymerized a precursor of the conjugated block and subsequently, after the incorporation of the second (coil) block, converted it into its conjugated form in a polymer-analogous reaction. While this method truly employs living polymerization techniques, any failure to achieve full conversion in the polymer-analogous reaction step leads to permanent defects in the conjugated block, which may adversely affect the photonic properties of the polymer.

A more versatile approach to the synthesis of (conjugated) rod–coil block copolymers is the use of an initiator for living polymerization that is attached to the rigid block. This enables one to synthesize a series of polymers with varying block length ratios from one batch of the conjugated block, which makes the comparison of different samples more straightforward. Moreover, this method allows the full characterization and purification of the conjugated block before its functionalization. Marsitzky et al. [56] demonstrated this approach recently, anionically grafting ethylene oxide from a polyfluorene block.

For the controlled formation of block copolymers with very low polydispersities, living anionic polymerization is certainly the most prominent method [57]. Drawbacks are the necessity to work under very strict conditions to avoid impurities such as water and oxygen, and restrictions with regard to functional groups [58]. Recently, this has been overcome to some extent by the development of the controlled/'living' radical polymerization techniques [59] using either stable nitroxide counter radicals [60,61] (nitroxide-mediated 'living' radical polymerization, NMRP) or atom transfer radical polymerization (ATRP) [62]. Their advantages are (a) compatibility with a wide variety of monomers, e.g. acrylates, styrenes, acrylonitrile, and derivatives, and (b) the possibility of characterizing intermediate products before reinitiating the polymerization in a different monomer solution to obtain block copolymers.

Our current strategy combines several of the more promising approaches mentioned above: we use controlled free radical polymerization to grow the coil block from an end-functionalized, substituted PPV block. We have chosen styrene as a monomer for the coil block, since it represents a well-investigated system. Accordingly, the acceptor C_{60} must be incorporated as a pendant group of a polystyrene backbone. In this study, this is accomplished via atom transfer radical addition (ATRA) to 4-chloromethylstyrene (CMS) repeat units [63]. Our work has demonstrated the benefits of employing a statistical copolymer of styrene and CMS in this procedure rather than a CMS homopolymer, to reduce crosslinking between multifunctional entities (C_{60}, polyCMS). At a styrene/CMS ratio of 2:1, the degree of functionalization with C_{60} should be sufficient to provide a continuous path for electrons (percolation). Hence, in our approach, styrene and CMS are the comonomers in the NMRP from a PPV-based macroinitiator. In addition to the aforementioned advantages of NMRP, radical polymerization does not interfere with either the olefinic double bonds of the PPV part, or the substituents on its phenyl rings. A similar methodology, yielding ABA block copolymers in a one-pot synthesis, was recently introduced by Klaerner et al. [64].

The synthesis of the monofunctionalized poly(1,4-(2,5-dioctyloxy)phenylene vinylene) (DOO-PPV) block is outlined in Fig. 1. Suitable conjugated blocks can be prepared along two approaches: (a) step-by-step synthesis of well-defined conjugated oligomers [49–51,65,66], or (b) one-step synthesis of conjugated polymers with relatively high, controllable molecular weight (around or above the effective conjugation length) and with relatively low polydispersity [52,53,64,67–74]. Although the oligomer route has the advantage of exact control of end-groups and molecular weight, it is extremely time-consuming for higher molecular weight polymers. Hence, we use the Siegrist [75,76] polycondensation technique, originally described by Kretzschmann and Meier [77,78], to obtain PPV blocks with exactly one aldehyde end-group. The subsequent attachment of the initiator to the rigid PPV block occurs via the nucleophilic attack of a Grignard reagent to the aldehyde group. An excess of the Grignard reagent guarantees complete functionalization, as was demonstrated by the disappearance of the aldehyde signal at 10.4 ppm in ^{1}H

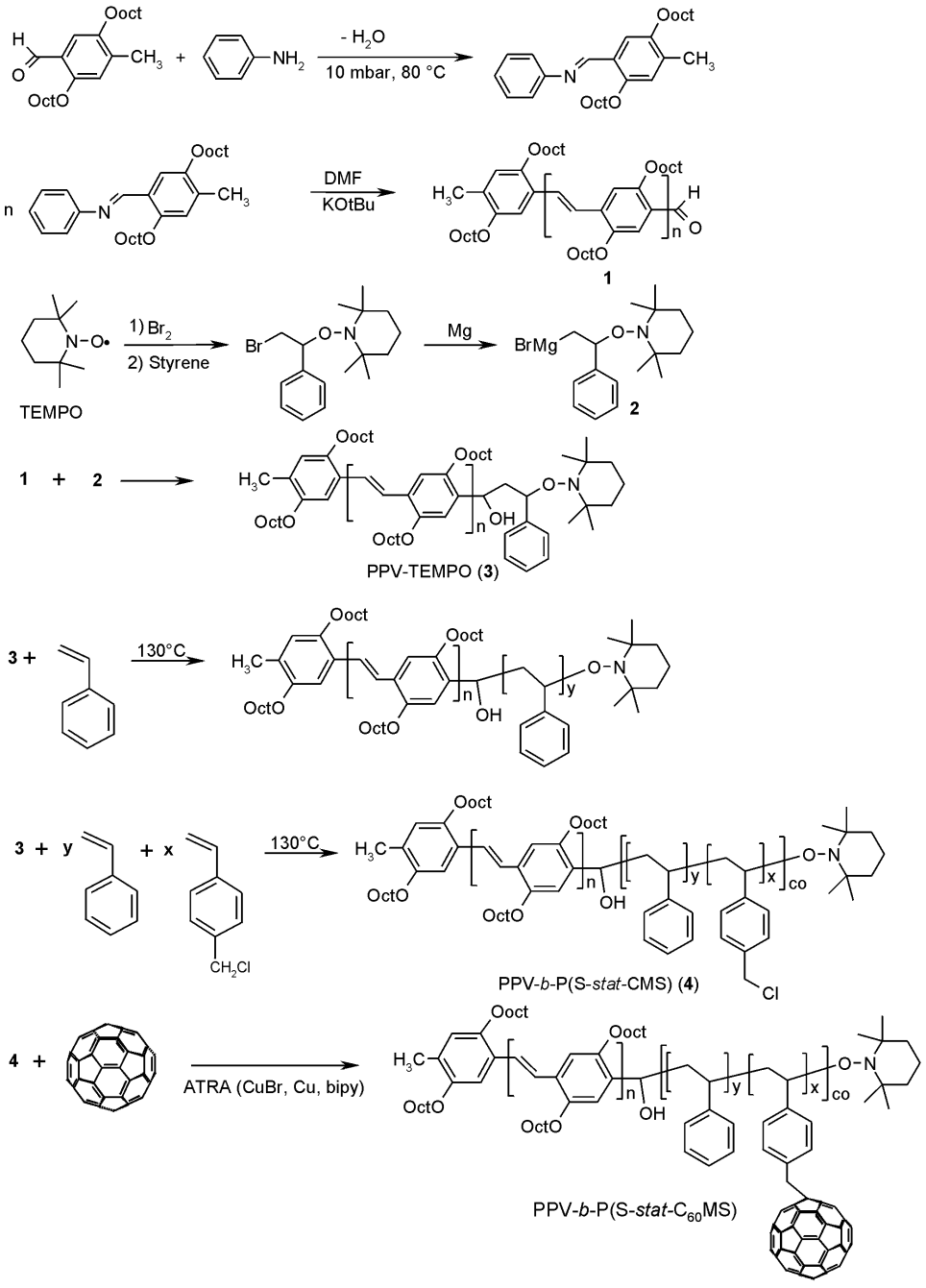

Fig. 1. Synthesis of DOO-PPV via Siegrist polycondensation, its subsequent functionalization with TEMPO initiator, the NMRP of styrene and the statistical copolymer of styrene and CMS, and the acceptor-functionalization of the block copolymer.

NMR, while the solubility of the initiator allows one to obtain the desired macroinitiator compound (PPV-TEMPO) by precipitation. The alkoxyamine initiator containing a bromide group for the formation of the Grignard reagent can be easily obtained by the reaction of TEMPO with Br_2, followed by the addition of styrene, as described by Kobatake et al. [79] and shown in Fig. 1 as well.

The average degree of polymerization of the PPV block can be determined either by end-group analysis with ^{1}H NMR or by UV–Vis spectroscopy. As ^{1}H NMR relies on the comparison of huge and small signals, it loses its accuracy with increasing molecular weight or when signals overlap. This analysis, based on the peaks of the methyl end-group at 2.2 ppm and the signals for the OCH_2 groups at 4.0 ppm, yielded an average degree of polymerization of 10 repeat units for the macroinitiator PPV-TEMPO. In a comparison of its UV–Vis spectrum with spectra of phenylene–vinylene oligomers [80], a length of seven repeat units was found from the absorption maximum at 467 nm, with

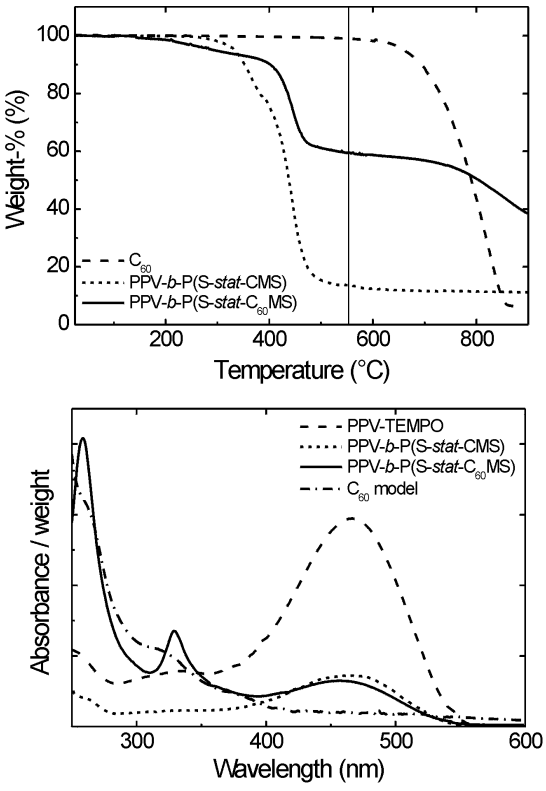

Fig. 2. Comparison of the starting diblock copolymer PPV-*b*-P(S-*stat*-CMS) (- - -) and the C_{60}-functionalized diblock copolymer PPV-*b*-P(S-*stat*-C_{60}MS) (—). Top: TGA, heating rate 10°C/min; the decomposition of C_{60} is shown for comparison (– – –). Bottom: UV–Vis absorption spectra in $CHCl_3$; the spectra of the PPV-TEMPO macroinitiator (– – –) and a C_{60}-containing model compound (–·–·) are shown for comparison.

clear indications of the presence of some higher oligomers. The latter was corroborated by GPC using UV detection. The calculations of the molecular weights of the entire block copolymers are based on a value of seven repeat units ($M_n = 2.5 \times 10^3$ g/mol) for the PPV block.

To investigate the 'living' character of the polymerization, the TEMPO-functionalized PPV block was used as a macroinitiator in NMRP of styrene, as depicted in Fig. 1. Samples of the PPV-*b*-PS system were taken after time intervals of 50, 95, and 105 min. Based on the (accurate) determination of block weight ratios from ^{1}H NMR end-group analysis (a comparison of the OCH_2 groups at 4.0 ppm with the aromatic contribution from polystyrene between 6.2 and 7.2 ppm), one calculates the molecular weight of the PS blocks to be 3.6, 6.3, and 7.0 kg/mol, respectively [63]. The solubility of the PPV block in the monomer solution limits the controlled polymerization of styrene by the PPV-based macroinitiator to a low conversion of styrene. At higher conversion, aggregates of the PPV blocks are formed during the reaction, resulting in a poor control over the molecular weight and polydispersity of the block copolymers. Nevertheless, increasing molecular weights with polymerization time are obtained. While GPC experiments also indicated an increase in molecular weight with conversion, those results cannot be used as absolute values due to the lack of appropriate standards for calibration.

Since it is our objective to bring PPV and C_{60} together in one molecule, we synthesized a statistical copolymer of styrene and CMS from our PPV-based macroinitiator. A feed ratio of styrene/CMS of 2:1 was chosen to prevent crosslinking and ensure solubility of the final, C_{60}-containing block copolymer. ^{1}H NMR analysis of the block copolymer indicated that the actual ratio of styrene to CMS is 1.5, and that the molecular weight of the styrenic block is 9 kg/mol. Subsequently, this block copolymer was functionalized with C_{60}. Fig. 2 shows TGA traces and UV–Vis spectra of the starting PPV-*b*-poly(S-*stat*-CMS) and the C_{60}-containing block copolymer. The increase in residue at 550°C from 14 to 60 wt% upon functionalization of the rod–coil block copolymer with C_{60} is very well visible in the TGA graph (Fig. 2, top). This indicates an average of 15 fullerene molecules per chain, and translates into one C_{60} for every two reactive sites in the starting polymer. In the bottom part of Fig. 2, weight-normalized absorption spectra are shown. The absorption band of the PPV block is centred around 465 nm. The C_{60}-functionalization by means of ATRA little affects the absorption band of the PPV block, indicating that the conjugation remains intact. A spectroscopic determination of the C_{60}-content of PPV-*b*-P(S-*stat*-C_{60}MS), using a C_{60}-containing model compound as the reference for a weight-normalized value of the absorbance at 330 nm, yields 45 wt% and agrees excellently with the TGA result [63].

3. Aggregation of PPV-based block copolymers in solution

The suitability of the block copolymers described above for application in photovoltaic devices relies, among other things, on the abilities of the respective blocks to function as electron donor and acceptor, and as charge transport media. As outlined above, the structure and morphology of the solid are crucial factors to both these functions. Both local order and morphology of a thin film obtained from a polymer solution by means of casting procedures will reflect the chain's microstructure, i.e. its conformation, entanglement topology, and the local order of aggregated segments, just prior to solidification or vitrification. The solidification process will proceed far from equilibrium conditions because of several factors, such as the temperature gradients caused by a rapid evaporation of solvent at the film surface, the accompanying concentration gradients and diffusive transport, and, in the case of spin-casting, bulk flow patterns. Admittedly, all these processes will certainly affect the microstructure during the transition from solution to solid film. The essential parameters governing the process may be assessed in first approximation, though only with

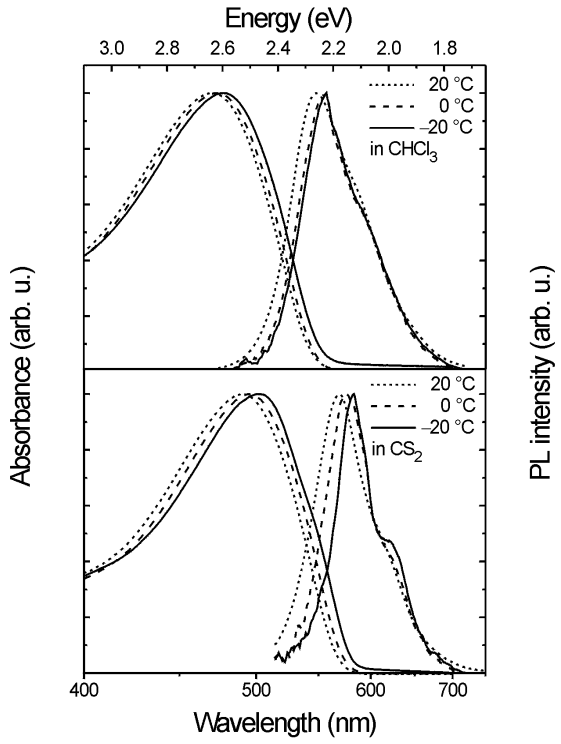

Fig. 3. UV–Vis absorption and PL spectra of PPV-*b*-PS as a function of temperature in chloroform and carbon disulfide.

caution, from a study of aggregation and solidification behaviour as a function of solvent quality and temperature under equilibrium conditions.

Aggregation in solutions of PPV-derivatives has been observed and the spectroscopic characteristics of the more common polymers (MEH-PPV, DOO-PPV) in various solvents as well as of the films produced from them have been quite extensively studied. Both temperature and solvent quality dramatically affect the wavelength (photon energy) of photoluminescence (PL) and the PL efficiency in solution [39,40,81] and affect the opto-electronic properties of the polymer film as well. For example, the luminescence from a solution of DOO-PPV in toluene was found to be gradually quenched upon cooling below room temperature, which was attributed to a strong reduction in solubility and the concomitant formation of aggregates [40]. The relative importance of intrachain and interchain (intersegment) interactions with respect to electronic excitations in polymer systems is still a topic of great interest as well as controversy [39,40,81–84].

In the case of diblock copolymers, the different solubilities of the two blocks in a given solvent will undoubtedly lead to a rich phase behaviour. In an environment that preferentially dissolves one of the blocks, we expect aggregation of the other block to give rise to the formation of micelles or even more complex mesophases [85]. In the DOO-PPV-based diblock copolymers described in this study, the PPV blocks could form the core of the micelles, and in view of their stiffness and restricted length, they might well form lyotropic nematic domains in specific solvents. The substitution pattern on the PPV block plays an important role in this respect.

3.1. Spectroscopic investigations

Fig. 3 shows the temperature dependence of the UV–Vis absorption and PL of $PPV_{3.9k}$-*b*-PS_{22k} in chloroform and in carbon disulfide. Clearly, in chloroform, both the absorption and fluorescence spectra do not change significantly upon cooling the solution from room temperature to −20°C, indicating that chloroform remains a fairly good solvent for the whole block copolymer chain over this temperature range. The slight red shift may be due to a reduction of thermal motions such as ring librations and hence a slight increase in conjugation (length).

Relative to the spectra in chloroform at the same temperature, the spectra obtained from solutions of the block copolymer in CS_2 are red-shifted. The temperature dependence of the peak wavelengths is slightly stronger in the latter solvent, but qualitatively similar. Since absorption and luminescence curves show equal shifts, these spectra are predominantly of single-molecule origin. Chain conformation adjustments as well as stabilization of the excited state by dipole rearrangements and induced-dipole effects are the likely cause of these thermochromic shifts and need not be elaborated upon here. The only remarkable feature is the emergence of an additional band around 630 nm upon cooling of the solution in CS_2. On the basis of additional results, to be described below, we attribute this peak to emission from an aggregated state. Since CS_2 dissolves polystyrene rather selectively, especially at lower temperatures, it seems reasonable to expect some form of aggregation of the PPV blocks.

Instead of employing different solvents, the quality of the medium can be varied by adding a poor solvent to a good solvent. Fig. 4 shows the results of increasing the fraction of acetone, a non-solvent for PPV, in a chloroform/acetone mixture containing 2×10^{-2} mg/ml PPV-*b*-PS. Since both these liquids are good solvents for polystyrene, one expects a much reduced solubility only for the PPV blocks in such a mixture. For a more detailed description, one would have to take preferential solvation into account, but this will be neglected in our discussion. The absorption spectra, little detailed as they are, broaden with increasing acetone content. While the maximum shifts slightly to the blue, the tail of the red edge moves out considerably. A blue shift is also observed for the fluorescence maximum initially at 540 nm; it moves about 0.07 eV. At higher acetone content, the fluorescence spectra have become more structured, and this is of great help in setting up the simplest model that is consistent with our results. Whereas the PL shoulders and maxima around 575 nm (2.15 eV) and 625 nm (1.98 eV) can be easily taken as belonging to the vibronic progression (of 0.17 eV), we think that such a

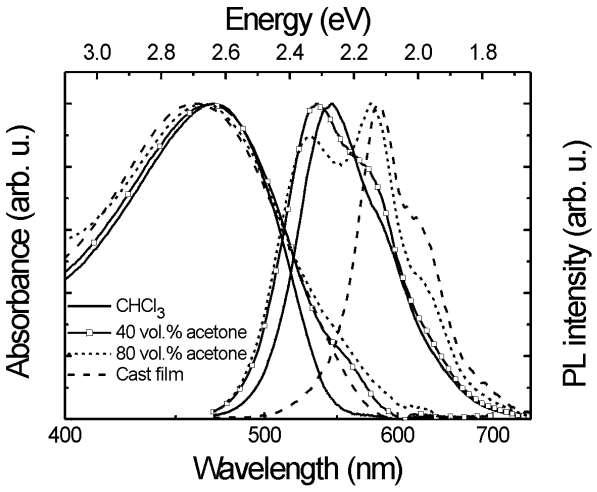

Fig. 4. UV–Vis absorption and PL spectra of PPV-*b*-PS in chloroform, in chloroform/acetone mixtures and as-cast film.

change in the Frank–Condon envelope is not plausible. We propose that these emerging features are actually a manifestation of a different species, an aggregate formed upon decreasing the solvent quality for the PPV block. This idea is supported by the spectrum obtained for the cast film: its PL has maxima at the aforementioned energies. Given the level of detail in the PL spectrum from this species, it is probably quite well defined from point of view of structure. The solution PL spectra are composites of single-molecule contributions (peaking around 540 nm) and aggregate contributions. This corroborates the idea of micelle formation, where such particles are in dynamic equilibrium with single molecules (unimers); the concentration of the latter remains fixed at the so-called critical micelle concentration. While a change in polymer concentration will merely change the number ratio between the two species, a change of the thermodynamic conditions may affect the structure and size of the micelle (see Section 3.2). The PL spectrum of the cast film has contributions from aggregate structures only. This does not imply that interchain arrangements are particularly uniform throughout this solid film, but ultrafast energy migration will ensure that the lowest-energy sites exclusively contribute to the PL. Not so for the absorption spectrum of the film, however, which is also broadened with respect to the spectrum from chloroform solution, and quite similar to the spectra from the mixed-solvent solutions. An extension on both the blue and the red sides of the single-molecule spectrum can be attributed to H-type aggregation and understood as modelled by Kasha et al. [86]. Dipole–dipole interactions in the excited state lead to a level splitting in which the higher level (blue-shifted) is one-photon allowed and the lower level (red-shifted) is one-photon forbidden. Any deviation from the strict H-type arrangement, or disorder, would introduce a finite transition probability from the ground state to the lower-level excited state. This would explain the tailing of the red edge of the absorption spectra. For the PL, the lower-lying aggregate state would be the only relevant state, because of ultra-fast internal conversion from the higher state. We note that inhomogeneous broadening due to disorder would be limited in the solid, as a result of energy diffusion. Since emission from the lower state has a low probability in H-type aggregates, it remains very relevant within the context of opto-electronic properties to measure the lifetime and quantum efficiency of this state [87], to assess the relative importance of the various possible deactivation pathways.

We have assessed the PL decay at 535, 585 and 630 nm upon excitation at a wavelength of 465 nm, using a Hamamatsu streak camera. All three experimental curves could be fitted well with a biexponential law. For each of the three wavelengths, we found similar time constants ($\tau_1 = 240 \pm 40$ ps, $\tau_2 = 710 \pm 20$ ps), and approximately equal weights as well. The spectral overlap between the two components has prevented us from making a more accurate determination of the individual contributions. Further experiments are necessary to resolve these components and to assess whether or not additional, weaker components are present.

3.2. Small-angle neutron scattering studies

For a further characterization of the aggregation behaviour of PPV-*b*-PS, we have used small-angle neutron scattering (SANS). The experiments were carried out at the pulsed neutron source at ISIS, UK [88]. In these experiments, we employed mixtures of deuterated chloroform and deuterated acetone to vary the solvent quality and we explored the range of 0–50 vol% acetone. To obtain practicable exposure times, a polymer concentration of 2 mg/ml (ca. 0.2 wt%) was used, which is 100 times as high as that for the spectroscopic measurements. With exposure times of 1.5–4 h per sample, the counting statistics are still moderate, especially at high $CDCl_3$ content, due to neutron absorption by chlorine. We have evaluated our data by fitting them to model curves calculated by means of the program FISH [89], assuming a spherical core–shell particle with an additional transition layer between core (PPV part of block copolymer molecules) and shell (PS blocks, swollen). The shell density has a ramp profile as well (Fig. 5). The results indicate an increase of both r_{inter} and r_{shell} with increasing acetone content. The size of the dense core (r_{core}) is probably around 2.5 nm; it is less well defined by the data, which have a usable scattering vector range $q = 0.1$–1.9 nm^{-1}. An additional measurement of a 0.1 wt% polymer solution in the 1:1 solvent mixture yielded dimensions similar to those found for the 0.2 wt% solution, which supports the idea of micelle formation. The calculated density contrasts are not entirely consistent yet with the simple picture of solid core and swollen shell. The discrepancy between measured data and fit at the smallest angles may indicate that a more elongated particle shape [90] or polydispersity is the source of

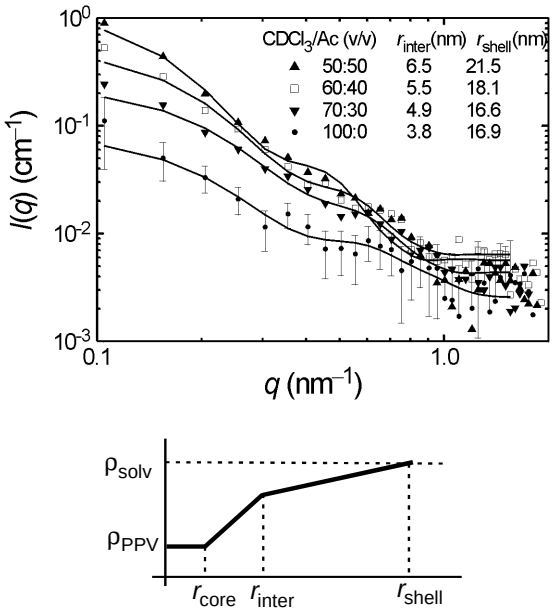

Fig. 5. Top: SANS data (log–log) of PPV-*b*-PS block copolymer in $CDCl_3$/acetone-d_6 mixtures (symbols), and model fits (lines). Bottom: density profile for the three-radii spherical-particle model used in fitting.

the deviations. The current data do not warrant more detailed modelling, however.

4. Self-organization of PPV-based block copolymer in solid films

It is our objective to reveal the relationships between the self-organization behaviour of our novel rod–coil block copolymers in selective solvents, the processing conditions, and the morphology of thin films thus produced. The results presented in Section 3 have demonstrated that changes in the thermodynamics of the environment result in quite complex and as yet unexplored behaviour of the rod–coil diblock copolymer chain. There are several clear indications of aggregate formation, accompanied by changes in the optical properties. The mesoscopic forms of self-organization are likely to be the 'nuclei' for solidification.

In this section, we will show that specific solution environments give rise to particular solid-state morphologies at various length scales. It is crucial to be able to interrelate these properties since the opto-electronic functionality that we are ultimately interested in, relies critically on a balance between intrachain and interchain electronic phenomena. In addition, phase morphology and higher levels of structuring, spanning several orders of magnitude in length scale, will affect the efficiencies of concurrent opto-electronic processes to different degrees. Hence, the processing history of the polymer is of decisive importance for its opto-electronic functionality. The fascinating results obtained so far demonstrate that this line of research is well worth pursuing.

4.1. Highly ordered hexagonal pattern on micrometre length scale

It was recently observed that rod–coil block copolymers and amphiphiles, cast from appropriate solvents as thin films on solid substrates, spontaneously form highly ordered, micro-porous honeycomb structures with a characteristic length scale [70,91–101]. These films, with pore sizes in the order of micrometres, may find applications in photonic and opto-electronic devices, catalysis, thermal insulation materials and membranes. Our PPV-based block copolymers are another prime example of this phenomenon [63,101]. Upon drop casting a 0.1 wt% solution of PPV-*b*-PS in CS_2 onto a glass slide in a flow-hood, we observed the condensation of water on the surface of the liquid film. After complete evaporation of the solvent, the samples revealed a highly ordered, two-dimensional, hexagonally close-packed air hole structure in the polymer film (Fig. 6). In optical transmission (top), the bright spots correspond to the cavities, which transmit the light completely. The fluorescence microscopy (bottom) reveals the honeycomb structure itself and indicates that the fluorescent block (PPV) is homogeneously distributed in the solid film.

Scanning electron microscopy (SEM) clearly displays the open surface structure of the polymer film with hole diameters of 2–3 μm and the presence of spherical cavities with a diameter of 3–5 μm (Fig. 6, bottom, inset). The SEM images also show that the cavities in the polymer film are mutually connected. However, it is not clear at the moment whether these connections are created during the preparation of the film for SEM imaging, or whether their occurrence is an intrinsic phenomenon in the formation of the polymer film.

We believe that the cavity pattern originates from the presence of water droplets, which at one stage form a two-dimensional uniform array [102]. The water condensation on the thin film of polymer solution and the subsequent water droplet formation, due to surface instabilities like Rayleigh–Bénard, Marangoni [103] or Bénard [104], which constitutes the template for the honeycomb formation, is the result of the cooling of the film surface during the evaporation of carbon disulfide. During the evaporation process, the surface reaches a minimum temperature of −6°C, as measured with an infrared thermometer. When CS_2 has evaporated completely, the water droplets have become immobilized in the polymer film. The sample then warms up, resulting in the expansion and subsequent evaporation of the encapsulated water droplets, after blistering the very thin top layer of the polymer film. This blistering process leaves behind a volcano-like structure at the polymer surface, as revealed with atomic force microscopy (AFM) (Fig. 6, top, inset). These remarkable structures have also been obtained for the D–A block copolymer PPV-*b*-P(S-*stat*-C_{60}MS) (Fig. 1) [63].

A highly ordered structure of this type can be utilized to trap solar light into the polymer layer by diffraction and

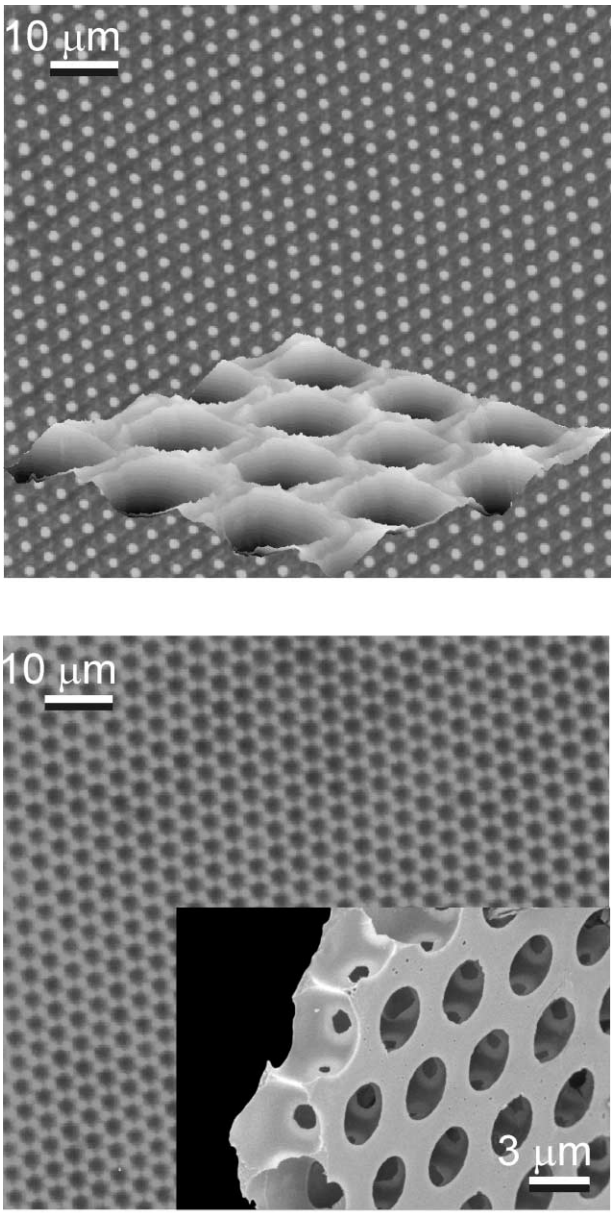

Fig. 6. Optical transmission and AFM (top), fluorescence and SEM (bottom) images of honeycomb-structured film as obtained by drop-casting of PPV-*b*-PS from CS_2.

guide the incident light into the polymer film, thus increasing the conversion efficiency of photovoltaic cells [105]. The spherical cavities will also decrease the reflection of non-perpendicular incoming light in photovoltaic devices. This concept was proven by forcing an elastomeric mould with a patterned grating on a thin polymeric film [105]. Using the spontaneously formed honeycomb structures would eliminate the additional processing step.

We found that the highly ordered honeycomb structure cannot be obtained via drop-casting from chloroform. One of the differences with a solution in CS_2 is that in the latter, aggregates may be formed at the lower temperatures reached during solvent evaporation, as indicated by our studies on solution behaviour described in Section 3. Because of the viscosity change accompanying it, aggregation in solution may play an essential part in the honeycomb self-structuring phenomenon.

4.2. Microphase separation of semiconducting block copolymers

Our spectroscopic studies show that PPV-*b*-PS exhibits a completely different behaviour in CS_2 than in chloroform. The differences in the chain conformation in solution are reflected in distinct morphologies of the polymer films. When the PPV-based block copolymers are cast from chloroform or *o*-dichlorobenzene, the resulting film exhibits a microphase-separated morphology but no higher-level structuring. Both PPV-*b*-PS and PPV-*b*-P(S-*stat*-C_{60}MS) give rise to similar microphase ordering (Fig. 7). AFM imaging in tapping mode on a spin-cast film revealed elongated domains of a fairly uniform thickness of approximately 15 nm. This size is compatible with a double layer of the PPV blocks. The AFM images do not resemble traditional images of highly ordered phase-separated coil–coil block copolymers. This is probably due to the rod-like character of the PPV block. Rod–coil polymers have been found to exhibit morphologies quite different from coil–coil polymers [42–44]. Moreover, we have observed that the homopolymer form of our conjugated block, with its symmetrically (dioctyloxy-) substituted phenylene–vinylene repeat units, exhibits a liquid-crystalline phase between 55 and 185°C, where the lower transition temperature is most likely related to side-chain melting. The presence of this mesogen may strongly influence the formation of the microdomains in the block copolymer [106]. The morphologies that we have obtained do not exhibit an ordered pattern and prompt us to study the phase behaviour in more detail. Still, our findings show that our first objective of inducing microphase separation in D–A block copolymers to control the scale of the interface between donor and acceptor moieties is feasible.

5. Photovoltaic response of D–A block copolymers

The incorporation of C_{60} moieties into one block of a diblock copolymer was aimed at satisfying two requirements for efficient operation as a photovoltaic material: (i) creating an accessible D–A interface at which dissociation of excitons into separate charge carriers is promoted, thus reducing the probability of decay along other routes, of which luminescence is one; (ii) providing separate pathways for transport of holes (via PPV) and electrons (via C_{60}), thus reducing the recombination probability. A reduction of the PL yield relative to the non-functionalized diblock copolymer is a first indication that an effective D–A interface has been created by incorporating the electron acceptor C_{60}. Fig. 8 shows the PL dynamics of films

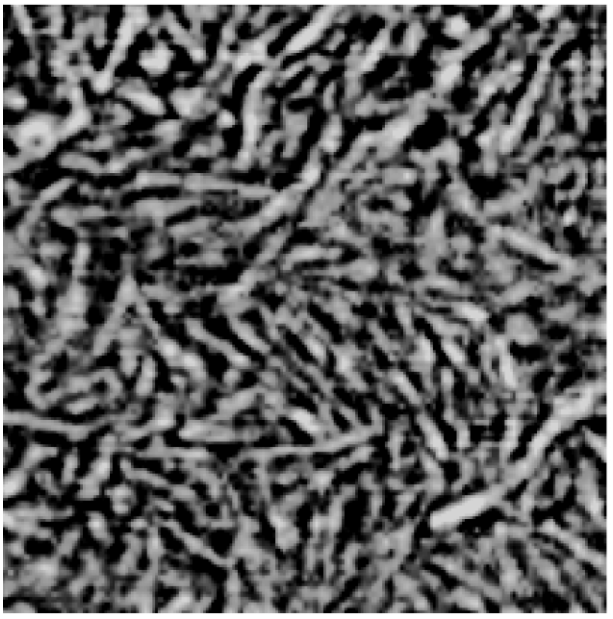

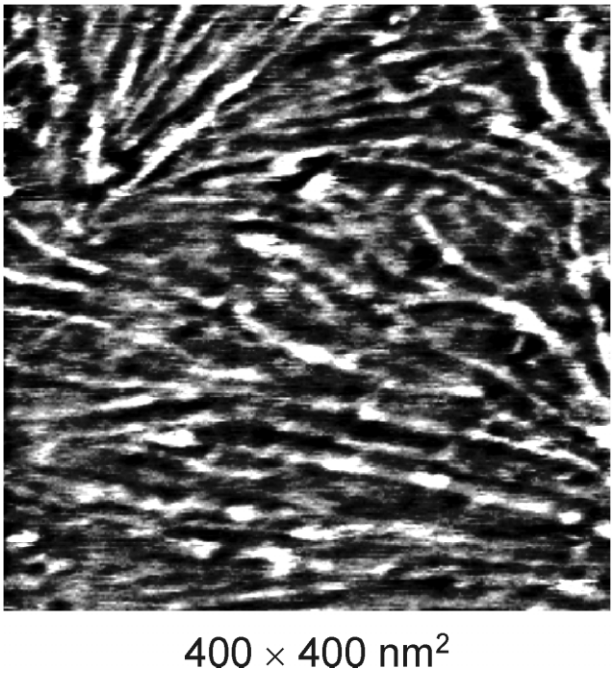

Fig. 7. The morphology of PPV-*b*-PS (top) and PPV-*b*-P(S-*stat*-C_{60}MS) (bottom) films spin-cast from solutions in *o*-dichlorobenzene, as imaged by tapping-mode AFM.

of PPV-*b*-P(S-*stat*-CMS) and PPV-*b*-P(S-*stat*-C_{60}MS). Whereas PPV-*b*-P(S-*stat*-CMS) exhibits long-lived PL extending into the nanosecond range, the PL decay time of the D–A block copolymer falls within the time resolution of our set-up (50 ps). With C_{60} incorporated, the PL intensity is reduced by three orders of magnitude. These results are taken as evidence for an efficient, very rapid electron

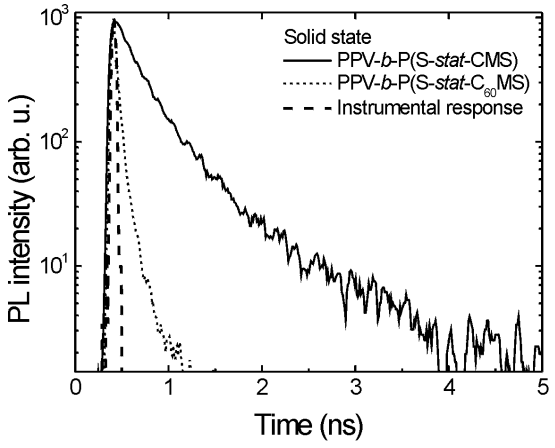

Fig. 8. PL decay of PPV-*b*-P(S-*stat*-CMS) (—) and PPV-*b*-P(S-*stat*-C_{60}MS) (- - -), and the instrumental response (– – –).

transfer from the donor block (PPV) to the acceptor (C_{60}). Both films exhibit similar morphologies, which makes the comparison legitimate.

As discussed above, the performance of a photovoltaic material is very sensitive to its morphology. In an ideal situation, when the morphologies are optimized in terms of exciton dissociation and charge transport, the photovoltaic performance of a D–A blend should be as good as that of the block copolymer based on the same donor and acceptor. The absence of any control over the phase separation in a blend, however, is likely to result in discontinuities of the donor and/or acceptor phases, because of the formation of isolated domains. In the case of the D–A block copolymer, even in the absence of any control, the length scale of phase separation will be much smaller. This increases the D–A interface relative to that of the blend and promotes the formation of continuous pathways for charges. Therefore, one should observe an enhancement of the photovoltaic response upon going from a blend of donor and acceptor homopolymers to the D–A block copolymer. In either system, mixing of donor and acceptor at the molecular scale may introduce increased energy level disorder in both phases, which results in an increase of the charge trap density and in a reduction of the electron and/or hole mobility.

Photovoltaic cells were fabricated by spin-casting a 1 wt% solution of polymer onto a poly(3,4-ethylenedioxythiophene)/poly(styrene sulphonate) (PEDOT/PSS) layer (70 nm) on ITO-covered glass substrates, resulting in a film thickness of approximately 100 nm. A 1:1 molar ratio blend of PPV homopolymer (seven repeat units) and a statistical copolymer P(S-*stat*-C_{60}MS) (with a S/C_{60}MS molar ratio of 2:1, $M_n = 17\,000$ g/mol) was compared with a block copolymer PPV-*b*-P(S-*stat*-C_{60}MS) (Fig. 1). Both blend and block copolymer contain the same amount of C_{60} and PPV to ensure that a direct comparison is meaningful. On top of the spin-cast films, a 100 nm thick

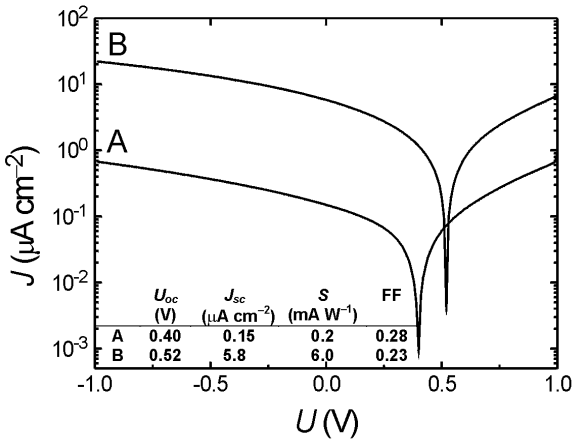

Fig. 9. Photovoltaic response of a PPV-*b*-P(S-*stat*-C_{60}MS) D–A block copolymer (B) compared with a blend of donor homopolymer and acceptor polymer (A) under monochromatic illumination of 458 nm. U_{oc}: open-circuit voltage, J_{sc}: short-circuit current density, S: sensitivity, FF: fill factor. The fill factor is defined as the maximum electrical power $(IV)_{max}$ that can be extracted from a photovoltaic diode divided by the product of maximum current I_{sc} and maximum voltage U_{oc}.

aluminium electrode was vapour-deposited to complete the sandwich-structured cell. The current versus voltage (I–V) curves of devices constructed from the blend and the block copolymer under monochromatic illumination of 1 mW/cm^2 at 458 nm are plotted in Fig. 9. It clearly demonstrates the superior response of the D–A block copolymer over the blend of the two constituent homopolymers. Characteristic parameters such as open-circuit voltage (U_{oc}), short-circuit current (I_{sc}) and sensitivity (S) are much better for the device based on the block copolymer. The open-circuit voltage, U_{oc}, is defined as the bias voltage at which the diode current becomes zero; the short-circuit current, I_{sc}, is the diode current at zero bias [31]. The photovoltaic sensitivity, S, is defined as the ratio of I_{sc} and the power of the incident light.

Based on a simple model of the metal–insulator–metal (MIM) diode and assuming both contacts to be neutral, one would expect the saturated open-circuit voltage to be approximately equal to the difference of the workfunctions of the two electrodes. Unlike the value of the Al workfunction, which is well accepted to be 4.3 eV, the value for a standard PEDOT/PSS layer is uncertain; according to published results, it is around 5.0 eV. Therefore, the measured open-circuit voltages correspond to the MIM model prediction. Although both blend and block copolymer show almost complete quenching of the fluorescence in the solid state, the obtained collection efficiencies (the ratio of collected electrons and absorbed photons) are significantly smaller than unity. This could be attributed to several processes among which the following two seem to be the most important ones. Firstly, exciton dissociation upon photoexcitation could be neither the only nor the main energy deactivation pathway. Energy transfer could compete with the dissociation, or the charge separation might not be effective. Secondly, the trap densities for electron and/or hole transport may be very high, resulting in a significant space-charge field. A verification of the exact mechanism requires an additional study on the electronic structure, charge transport and photophysics of the blend and the block copolymer.

The results presented above, obtained on materials that still leave ample room for optimization as far as microstructure is concerned, seem to validate our strategy towards composite materials for photovoltaic applications, as outlined in Section 1.

6. Concluding remarks and outlook

Structuring at the nanometre level is one of the features of functional materials of the new generation, including, but not limited to, opto-electronic materials. Most efficiently and elegantly, this structuring should be accomplished through self-organization of matter rather than by manipulation or machining, wherever possible. The idea seems to be highly applicable to block copolymers, which can be chemically fine-tuned to show phase separation at the proper scale and to possess the desired chemical, physical and electronic properties.

We have succeeded in making a diblock copolymer PPV-*b*-P(S-*stat*-C_{60}MS) with each block having an electronic function, and we have confirmed some of its targeted, photovoltaic characteristics. Its structuring behaviour in solution (aggregates) and in the solid (at nano- and micrometre scales) has been revealed. Many aspects still require optimization, and because of the rod–coil nature of the macromolecule, this must proceed in a largely unexplored region of parameter space. This task may be intimidating, but then again rewarding too, as novel phenomena are discovered.

With chemical routes towards conjugated polymers being so different from those employed for conventional polymers, synthetic chemists face an enormous challenge in dealing with block copolymer architectures. The introduction of block copolymers, however, into the arena of organic opto-electronics will give well-established polymer science an opportunity to make its long-awaited, substantial contribution to this vibrant field.

Acknowledgements

The following people are gratefully acknowledged for their contribution to the work described: G.O.R. Alberda van Ekenstein, M. van den Boogaard, H. Nijland, E.K. Schäffer, C. Videlot, E.J. Vorenkamp (Department of Polymer Chemistry); S.M. King (ISIS, Rutherford Appleton Laboratory, Chilton, UK). We thank NWO-CW, NWO-STW, FOM, and the EU for financial support.

References

[1] Chiang CK, Fincher CR, Park YW, Heeger AJ, Shirakawa H, Louis EJ, Gau SC, MacDiarmid AG. Phys Rev Lett 1977;39:1098–101.
[2] Shirakawa H, Louis EJ, MacDiarmid AG, Chiang CK, Heeger AJ. J Chem Soc, Chem Commun 1977:578–80.
[3] Burroughes JH, Bradley DDC, Brown AR, Marks RN, MacKay K, Friend RH, Burn PL, Holmes AB. Nature 1990;347:539–41.
[4] Bao Z. Adv Mater 2000;12:227–30.
[5] Horowitz G. Adv Mater 1998;10:365–77.
[6] Crone B, Dodabalapur A, Lin Y-Y, Filas RW, Bao Z, LaDuca A, Sarpeshkar R, Katz HE, Li W. Nature 2000;403:521–3.
[7] Friend RH, Gymer RW, Holmes AB, Burroughes JH, Marks RN, Taliani C, Bradley DDC, Dos Santos DA, Brédas JL, Lögdlund M, Salaneck WR. Nature 1999;397:121–8.
[8] Kraft A, Grimsdale AC, Holmes AB. Angew Chem Int Ed 1998;37:402–28.
[9] Bernius MT, Inbasekaran M, O'Brien J, Wu W. Adv Mater 2000;12:1737–50.
[10] Ho PKH, Kim J-S, Burroughes JH, Becker H, Li SFY, Brown TM, Cacialli F, Friend RH. Nature 2000;404:481–4.
[11] Yu G, Wang J, McElvain J, Heeger AJ. Adv Mater 1998;10:1431–4.
[12] Sariciftci NS, Smilowitz L, Heeger AJ, Wudl F. Science 1992;258:1474–6.
[13] Sariciftci NS, Braun D, Zhang C, Srdanov VI, Heeger AJ, Stucky G, Wudl F. Appl Phys Lett 1993;62:585–7.
[14] Yu G, Gao J, Hummelen JC, Wudl F, Heeger AJ. Science 1995;270:1789–91.
[15] Granström M, Petritsch K, Arias AC, Lux A, Andersson MR, Friend RH. Nature 1998;395:257–60.
[16] Chen L, McBranch DW, Wang H, Helgeson R, Wudl F, Whitten DG. Proc Natl Acad Sci USA 1999;96:12287–92.
[17] Moses D. Appl Phys Lett 1992;60:3215–6.
[18] Hide F, Schwartz BJ, Díaz-García MA, Heeger AJ. Chem Phys Lett 1996;256:424–30.
[19] Hide F, Díaz-García MA, Schwartz BJ, Andersson MR, Pei Q, Heeger AJ. Science 1996;273:1833–6.
[20] Schön JH, Kloc Ch, Dodabalapur A, Batlogg B. Science 2000;289:599–601.
[21] McGehee MD, Heeger AJ. Adv Mater 2000;12:1655–68.
[22] Drury CJ, Mutsaers CMJ, Hart CM, Matters M, de Leeuw DM. Appl Phys Lett 1998;73:108–10.
[23] Renak ML, Bazan GC, Roitman D. Synth Met 1998;97:17–21.
[24] Hebner TR, Wu CC, Marcy D, Lu MH, Sturm JC. Appl Phys Lett 1998;72:519–21.
[25] Chang S-C, Liu J, Bharathan J, Yang Y, Onohara J, Kido J. Adv Mater 1999;11:734–7.
[26] Sirringhaus H, Kawase T, Friend RH, Shimoda T, Inbasekaran M, Wu W, Woo EP. Science 2000;290:2123–6.
[27] Granlund T, Nyberg T, Stolz Roman L, Svensson M, Inganäs O. Adv Mater 2000;12:269–73.
[28] Pschenitzka F, Sturm JC. Appl Phys Lett 1999;74:1913–5.
[29] Rogers JA, Bao Z, Dhar L. Appl Phys Lett 1998;73:294–6.
[30] Gustafsson G, Cao Y, Treacy GM, Klavetter F, Colaneri N, Heeger AJ. Nature 1992;357:477–9.
[31] Wöhrle D, Meissner D. Adv Mater 1991;3:129–38.
[32] Brédas JL, Cornil J, Heeger AJ. Adv Mater 1996;8:447–52.
[33] Smilowitz L, Sariciftci NS, Wu R, Gettinger C, Heeger AJ, Wudl F. Phys Rev B 1993;47:13835–42.
[34] Helfand E, Wasserman ZR. In: Goodman I, editor. Developments in block copolymers — 1. New York: Applied Science, 1982. p. 99–125.
[35] Bates FS, Fredrickson GH. Annu Rev Phys Chem 1990;41:525–57.
[36] Bates FS. Science 1991;251:898–905.
[37] Jenekhe SA, Chen XL. J Phys Chem B 2000;104:6332–5.
[38] Chen XL, Jenekhe SA. Macromolecules 2000;33:4610–2.
[39] Nguyen T-Q, Doan V, Schwartz BJ. J Chem Phys 1999;110:4068–78.
[40] Hsu J-H, Fann W, Tsao P-H, Chuang K-R, Chen S-A. J Phys Chem A 1999;103:2375–80.
[41] Yu L, Bao Z. Adv Mater 1994;6:156–9.
[42] Matsen MW, Barrett C. J Chem Phys 1998;109:4108–18.
[43] Lee M, Cho B-K, Kang Y-S, Zin W-C. Macromolecules 1999;32:7688–91.
[44] Chen JT, Thomas EL, Ober CK, Mao G-P. Science 1996;273:343–6.
[45] Brabec CJ, Sariciftci NS. In: Hadziioannou G, van Hutten PF, editors. Semiconducting polymers — chemistry, physics and engineering. Weinheim: Wiley/VCH, 2000. p. 515–60.
[46] Brabec CJ, Padinger F, Hummelen JC, Janssen RAJ, Sariciftci NS. Synth Met 1999;102:861–4.
[47] Geckeler KE, Samal S. Polym Int 1999;48:743–57.
[48] Chen Y, Huang Z-E, Cai R-F, Yu B-C. Eur Polym J 1998;34:137–51.
[49] Hempenius MA, Langeveld-Voss BMW, van Haare JAEH, Janssen RAJ, Sheiko SS, Spatz JP, Möller M, Meijer EW. J Am Chem Soc 1998;120:2798–804.
[50] Li W, Wang H, Yu L, Morkved TL, Jaeger HM. Macromolecules 1999;32:3034–44.
[51] Tew GN, Pralle MU, Stupp SI. J Am Chem Soc 1999;121:9852–66.
[52] Jenekhe SA, Chen XL. Science 1998;279:1903–7.
[53] Marsitzky D, Brand T, Geerts Y, Klapper M, Müllen K. Macromol Rapid Commun 1998;19:385–9.
[54] Kukula H, Ziener U, Schöps M, Godt A. Macromolecules 1998;31:5160–3.
[55] Leclère PH, Parente V, Brédas JL, François B, Lazzaroni R. Chem Mater 1998;10:4010–4.
[56] Marsitzky D, Klapper M, Müllen K. Macromolecules 1999;32:8685–8.
[57] Szwarc M. J Polym Sci, Part A: Polym Chem 1998;36:ix–xv.
[58] Dasgupta A, Sivaram S. JMS, Rev Macromol Chem Phys 1997;C37:1–59.
[59] Baumert M, Frey H, Hölderle M, Kressler J, Sernetz FG, Mülhaupt R. Macromol Symp 1997;121:53–74.
[60] Malmström EE, Hawker CJ. Macromol Chem Phys 1998;199:923–35.
[61] Hawker CJ. Acc Chem Res 1997;30:373–82.
[62] Patten TE, Matyjaszewski K. Adv Mater 1998;10:901–15.
[63] Stalmach U, de Boer B, Videlot C, van Hutten PF, Hadziioannou G. J Am Chem Soc 2000;122:5464–72.
[64] Klaerner G, Trollsås M, Heise A, Husemann M, Atthoff B, Hawker CJ, Hedrick JL, Miller RD. Macromolecules 1999;32:8227–9.
[65] Li W, Maddux T, Yu L. Macromolecules 1996;29:7329–34.
[66] Tew GN, Pralle MU, Stupp SI. Angew Chem Int Ed 2000;39:517–21.
[67] Zhong XF, François B. Synth Met 1989;29:E35–40.
[68] Zhong XF, François B. Makromol Chem 1991;192:2277–91.
[69] François B, Olinga T. Synth Met 1993;55–57:3489–94.
[70] François B, Widawski G, Rawiso M, Cesar B. Synth Met 1995;69:463–6.
[71] Osaheni JA, Jenekhe SA. J Am Chem Soc 1995;117:7389–98.
[72] Francke V, Räder HJ, Geerts Y, Müllen K. Macromol Rapid Commun 1998;19:275–81.
[73] Bianchi C, Cecchetto E, François B. Synth Met 1999;102:916–7.
[74] Mignard E, Tachon C, François B. Synth Met 1999;102:1246–7.
[75] Siegrist AE, Liechti P, Meyer HR, Weber K. Helv Chim Acta 1969;52:2521–54.
[76] Siegrist AE. Helv Chim Acta 1981;64:662–80.
[77] Meier H, Kretzschmann H, Lang M. J Prakt Chem 1994;336:121–8.
[78] Kretzschmann H, Meier H. Tetrahedron Lett 1991;32:5059–62.
[79] Kobatake S, Harwood HJ, Quirk RP, Priddy DB. Macromolecules 1999;32:10–13.
[80] Meier H, Stalmach U, Kolshorn H. Acta Polymer 1997;48:379–84.

[81] Nguyen T-Q, Martini IB, Liu J, Schwartz BJ. J Phys Chem B 2000;104:237–55.
[82] Samuel IDW, Crystall B, Rumbles G, Burn PL, Holmes AB, Friend RH. Chem Phys Lett 1993;213:472–8.
[83] Blatchford JW, Jessen SW, Lin L-B, Gustafson TL, Fu D-K, Wang H-L, Swager TM, MacDiarmid AG, Epstein AJ. Phys Rev B 1996;54:9180–9.
[84] Schwartz BJ, Hide F, Andersson MR, Heeger AJ. Chem Phys Lett 1997;265:327–33.
[85] Wang H, Wang HH, Urban VS, Littrell KC, Thiyagarajan P, Yu L. J Am Chem Soc 2000;122:6855–61.
[86] Kasha M, Rawls HR, Ashraf El-Bayoumi M. Pure Appl Chem 1965;11:371–92.
[87] Chang R, Hsu JH, Fann WS, Yu J, Lin SH, Lee YZ, Chen SA. Chem Phys Lett 2000;317:153–8.
[88] King SM. Small-angle neutron scattering. In: Pethrick RA, Dawkins JV, editors. Modern techniques for polymer characterisation. Wiley: Chichester, 1999. p. 171–232.
[89] Heenan RK. The FISH reference manual (data fitting program for small-angle diffraction, etc.). RAL Report 89-129 (revised 6/11/2000).
[90] Urban V, Wang HH, Thiyagarajan P, Littrell KC, Wang HB, Yu L. J Appl Cryst 2000;33:645–9.
[91] Widawski G, Rawiso M, François B. Nature 1994;369:387–9.
[92] François B, Pitois O, François J. Adv Mater 1995;7:1041–4.
[93] Pitois O, François B. Colloid Polym Sci 1999;277:574–8.
[94] Pitois O, François B. Eur Phys J B 1999;8:225–31.
[95] Jenekhe SA, Chen XL. Science 1999;283:372–5.
[96] Maruyama N, Koito T, Nishida J, Sawadaishi T, Cieren X, Ijiro K, Karthaus O, Shimomura M. Thin Solid Films 1998;327:854–6.
[97] François B, Ederlé Y, Mathis C. Synth Met 1999;103:2362–3.
[98] Mourran A, Sheiko SS, Möller M. Proc ACS PMSE 1999;81:18–19.
[99] Shimomura M, Koito T, Maruyama N, Arai K, Nishida J, Gråsjö L, Karthaus O, Ijiro K. Mol Cryst Liq Cryst 1998;322:305–12.
[100] Karthaus O, Maruyama N, Cieren X, Shimomura M, Hasegawa H, Hashimoto T. Langmuir 2000;16:6071–6.
[101] de Boer B, Stalmach U, Nijland H, Hadziioannou G. Adv Mater 2000;12:1581–3.
[102] Govor LV, Bashmakov IA, Kaputski FN, Pientka M, Parisi J. Macromol Chem Phys 2000;201:2721–8.
[103] Bestehorn M. Phys Rev E 1993;48:3622–34.
[104] Schatz MF, VanHook SJ, McCormick WD, Swift JB, Swinney HL. Phys Rev Lett 1995;75:1938–41.
[105] Stolz Roman L, Inganäs O, Granlund T, Nyberg T, Svensson M, Andersson MR, Hummelen JC. Adv Mater 2000;12:189–95.
[106] Leclère Ph, Calderone A, Marsitzky D, Francke V, Geerts Y, Müllen K, Brédas JL, Lazzaroni R. Adv Mater 2000;12:1042–6.